

DESIGN OF A CORRELATOR IN SOFTWARE FOR SYNTHESIS IMAGING WITH A RADIO ASTRONOMY TELESCOPE ARRAY

*A Postgraduate Project Report submitted to Manipal University in partial
fulfilment of the requirement for the award of the degree of*

MASTER OF TECHNOLOGY

In

Digital Electronics and Advanced Communication

Submitted by

Rahul Suresh Kinger

(130915009)

Under the guidance of

Avinash Deshpande

Professor

Raman Research Institute

&

HS Mruthyunjaya

Professor

Manipal Institute of Technology





DEPARTMENT OF ELECTRONICS AND COMMUNICATIONS ENGINEERING

MANIPAL INSTITUTE OF TECHNOLOGY

(A Constituent College of Manipal University)

MANIPAL – 576104, KARNATAKA, INDIA

Aug 2015



DEPARTMENT OF ELECTRONICS AND COMMUNICATIONS ENGINEERING
MANIPAL INSTITUTE OF TECHNOLOGY
(A Constituent College of Manipal University)
MANIPAL – 576 104 (KARNATAKA), INDIA

Manipal
20th Aug 2015

CERTIFICATE

This is to certify that the project titled **DESIGN OF A CORRELATOR IN SOFTWARE FOR SYNTHESIS IMAGING WITH A RADIO ASTRONOMY TELESCOPE ARRAY** is a record of the bonafide work done by **RAHUL SURESH KINGER** (Reg. No. 130915009) submitted in partial fulfilment of the requirements for the award of the Degree of Master of Technology (M.Tech) in **DIGITAL ELECTRONICS AND ADVANCED COMMUNICATION** of Manipal Institute of Technology Manipal, Karnataka, (A Constituent College of Manipal University), during the academic year 2014-15.

Prof. Dr. HS Mruthyunjaya

Prof. Dr.Somashekara Bhat

Project Guide

*HOD, ECE Dept.
M.I.T, MANIPAL*

रामन अनुसंधान संस्थान

सी. वी. रामन एवेन्यू, सदशिवनगर, बेंगलूर - 560 080, भारत

RAMAN RESEARCH INSTITUTE

C. V. Raman Avenue, Sadashivanagar, Bangalore - 560 080, India



Prof. A.A. Deshpande
Astronomy and Astrophysics

August 7, 2015

To whomsoever it may concern

This is to certify that Rahul Suresh Kinger (Reg. No. 130915009) has been working with me on a project entitled "*Design of a correlator in software for synthesis imaging with a radio astronomy telescope array*" since July 2014.

A. A. Deshpande

ACKNOWLEDGMENT

I owe thanks to many people who helped and supported me during the successful completion of this project.

I express my sincere thanks to Avinash Deshpande (Desh), Professor, RRI, for giving me an opportunity to work with him and teach me the many aspects of Signal Processing and Radio Astronomy with utmost dedication and patience. I extend my gratitude to all the members of the Radio Astronomy Lab for having taken time to teach me and guide me through my work. I would also like to thank some of the visiting students who were a part of the discussions which helped me with my work.

Many thanks to Dr. HS Mruthyunjaya, Professor, E&C Department, Manipal Institute of Technology for having kept a track of my work and for all the guidance and necessary corrections he made for my project.

I express my heartfelt gratitude to Dr.Somashekara Bhat, Professor & HOD of E&C Department, Manipal Institute of Technology and Dr. Satish Kumar, Professor & DEAC course co-ordinator for responding promptly and enthusiastically to my requests, despite his congested schedule.

Finally, I thank my Institution, Manipal Institute of Technology, Manipal, and also my family and friends.

Contents			Page No
List Of Figures			1
Chapter 1			
INTRODUCTION			2
1.	Objective		2
1.	Motivation of the Project		2
2			
Chapter 2			
LITERATURE REVIEW			3
2.	Radio Astronomy		3
1			
2.	Interferometry		4
2			
	2.2.1	Young's Double Slit Experiment	5
	2.2.2	Michelson's Interferometer	6
	2.2.3	A Simple Two Element Antenna Interferometer	7
2.	Relationship Between Intensity and Visibility		8
3			
	2.3.1	Delay Tracking	10
2.	Antenna Array Telescope		12
4			
2.	Earth Rotation Synthesis		13
5			
2.	Polarimetry		14
6			
Chapter 3			
RESEARCH METHODOLOGY AND EXPERIMENTAL SETUP			18
3.1	Experimental Setup		18
	3.1.1	Murchison Wide-field Array Antennae (MWA)	18
	3.1.2	The Beam Former with the MWA	20
	3.1.3	The Multi Band Receiver System (MBR)	21
	3.1.4	The MBR software system	22
3.2	Software Correlator System Being Developed		23
	3.2.1	Calibration technique for system and cable delays	26
	3.2.2	Local Sidereal Time	27
	3.2.3	Coordinate Systems	27
	3.2.4	The Dirty map and the Dirty Image	29
	3.2.5	Some Challenges	29
Chapter 4			
RESULT ANALYSIS			31
Chapter 5			
CONCLUSION AND FUTURE SCOPE			37

LIST OF FIGURES

Figure No	Figure Title	Page No
1	Illustration of Young's Double Slit Experiment	5
2a.	Michelson-Pease Stellar Interferometer Setup	7
2b.	Michelson-Pease Stellar Interferometer Intensity of image as a function of position angle	8
3	A simple two element interferometer	10
4	Baseline and source position vectors that specify the interferometer and source	13
5a.	Schematic of a Phased Array	14
5b.	Schematic of a Correlator Array	15
6	Block Diagram of the SWAN system	18
7	An MWA antenna tile image with a Beamformer	19
8a	Block diagram of an FX correlator being used in the GMRT array	25
8b	Implementation of the FX style correlator being used in the GMRT array	26
9a	Plot of amplitudes and phases of cross products as a function of frequency	31
9b	Plot of amplitudes and phases of cross products as a function of time	32
10a	Delay cross correlation plot before calibration	33
10b	Delay cross correlation plot after calibration	34
10c	Post calibration plot of amplitudes and phases of cross products as a function of frequency	34
11a	Dirty Map representation for a baseline	35
11b	Dirty Beam representation for the baselines as seen in the Dirty Map	35
12	A dirty phase suppressed image of the Sun at mid band	36

CHAPTER 1

INTRODUCTION

1.1 OBJECTIVE

To develop a correlator in software for a radio astronomical array of telescopes and construct an image of the source.

1.2 MOTIVATION OF THE PROJECT

Currently many of the Radio Astronomical telescopes are using FPGAs to correlate signals for synthesis of an aperture. These circuits are highly customized and are specific to an application, and making a change at this stage may require redesigning and rework. Hence to make things more flexible, the cross correlations including the various compensations for imaging, are taken care of in software.

The part up to digitizing and packetizing of the signal information are handled by FPGAs and after this point on we will depend on software entirely for synthesizing the image of the source of interest.

Sky Watch Area Network (or SWAN) is a project proposed in order to achieve some basic goals such as:-

1. Creating large baselines by utilizing locations across India (of the order of 3000km or the length of the country), to obtain very fine angular resolution in the Low frequency radio range of 80MHz to 300MHz initially and later it is desired to extend this from 50MHz to 500MHz. These locations may not necessarily be free of Radio Frequency Interference (RFI), unlike other radio telescopes around the world.
2. To create a system which is capable of making fast correlations in Real Time that can be implemented in software, so that they can be used to track Pulsars and other Fast Radio Bursts (FRBs) which usually occur within timescales of the order of a millisecond.

CHAPTER 2

LITERATURE SURVEY

2.1 RADIO ASTRONOMY

Radio Astronomy is a branch of astronomy that deals with studying the relatively lower range of frequencies that lie in the Radio region of the electromagnetic spectrum, which typically extends from a few MHz to few hundred GHz. Unlike optical telescopes that capture frequencies in the visible range of the spectrum that have frequencies in the range of THz, these signals incident on a radio telescope cannot be viewed directly and can only be digitized, recorded and processed in a manner that can be comprehended with the help of imaging techniques with pseudo coloring.

Radio Astronomy also differs from Optical (as well as Infrared and Ultraviolet) astronomy in the aspect that Optical telescopes consist of photo-detectors that are basically reverse biased diodes that generate a reverse current proportional to the intensity of light shining on their surface. Although photon densities are very low in the optical range, the individual photon energies are high enough to generate a detectable current. This is not the same for the radio frequency range where the individual photon energies are very low and cannot generate reverse current in a photo detector, however the photon densities are usually high at this range and this can be exploited to our advantage. A metallic structure called an antenna, whose size is of the order of the wavelength of the radio frequency that one wishes to observe, are employed. When radio frequency is incident on the surface of the metal, it makes the free electrons in the metal oscillate with the same frequency as that of the electric field in the incident radio wave. A current and hence a voltage gets produced in the metal and this voltage is proportional to the incident electric field, which can be recorded in digital format via an Analog to Digital Converter (ADC).

A major advantage that Radio has over other waves, is that ground based observations on the earth are possible using Radio wavelengths as they do not get absorbed by the Earth's atmosphere as most other wavelengths do.

In the optical spectrum, the diffraction limit of large telescopes (with diameter approx 8m), is about 0.015 arc-second, but the angular resolution possible by observing from the surface of the earth degrades to about 1 arc-second which is due to turbulence in the troposphere. So,

for progress in astronomy, it is important to measure positions of the radio sources with sufficient accuracy to allow identification with the objects detected in the optical and other regions of the electromagnetic spectrum [1].

The formation of our universe is dated to about 13.2 billion years ago as per the Big Bang model and it is believed that right after the big bang, the universe generated the invisible Cosmic Microwave Background Radiation. The universe since its formation has been expanding and objects are moving away from each other, which translate as a red-shift in wavelengths that are emanating from objects as per the Doppler shift principle and this has resulted in radiations being emitted in the radio range.

In some sense, by looking at these long wavelengths, we are in fact looking into the past and by studying these, we can attempt to understand the formation of the objects in our universe like stars, Pulsars, Black holes, etc.

2.2. INTERFEROMETRY

Using a single radio telescope antenna puts a limit on the angular resolution of the objects that can be observed, since the Angular Resolution of the Source is the ratio of observed Wavelength (λ) upon Diameter of the telescope (D) used to observe the source, $R = \lambda / D$ (where R = resolution is in radians). Typically a resolution of the order of arc-seconds or less is desired to observe sources and making some inference about their structure. This requires the size of the antenna aperture to be very large.

Suppose we wish to observe a band of frequencies centered at 100MHz. The center wavelength is at 3m, which means that to be able to achieve 1 arc-second resolution, we need an aperture size of about 620km and the construction of a single such large aperture is extremely impractical. The observatory at Arecibo currently hosts the world's largest single aperture antenna with an aperture size of 305m.

To be able to create large apertures without the high costs of construction and sophisticated mechanical rotation to track sources as in a single aperture structure, we can utilize many

smaller apertures spread out over a larger area and stitch large apertures. This invokes the basic principle of an interference pattern produced by two waves interfering with each other.

2.2.1 Young's Double Slit experiment

Before we can venture further into Interferometry, we must understand the basic principle of an interferometer and how it can be applied to radio telescopes. We consider the Young's experiment as a starting point in building our understanding towards the same.

A monochromatic light source was made to fall on surface which has two slits. This caused diffracted light out of the slits to interfere with each other on the screen and create a diffraction pattern. The pattern consists of light and dark regions which are caused by constructive and destructive phase interference of the two waves.

A line projected from the center of the slits towards the screen corresponds to the central bright maxima, and on either sides of it will be the minima which are at half wavelength distance, which correspond to the destructive interference between the waves from the two slits, and at a full wavelength on either sides will lie the next maxima point which will not be as bright as the central maxima, owing to the fact that the diffraction caused by the slits is having a narrow spread, and eventually the pattern will fade out on either sides.

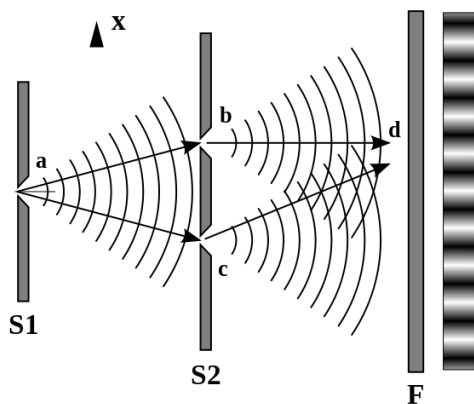


Fig.1. Illustration of Young's double slit experiment. The two slits will now act as individual sources and will send out the waves with a spherical wave front. If the concentric wave fronts denote the maxima then where two lines interfere will correspond to a constructive interference.

If the radiation is not monochromatic, then the central bright fringe will still remain due to constructive interference but the subsequent adjacent maxima will start to interfere destructively and will begin to fade out (this can be imagined from the principle of superposition applied to the different wavelengths present). So eventually we will be able to only view the direction corresponding to the central (bright) white fringe, which is the overhead direction. The angle around the center for which the source with a finite bandwidth may be viewed can be given by the diffraction equation as,

$$\theta = \sin^{-1} (c/d\Delta\nu),$$

Where, $\Delta\nu$ is the bandwidth, d is the physical separation between the slits; c is the speed of light in vacuum.

2.2.2 Michelson's interferometer

Michelson's apparatus for interferometer is as shown in Fig. 2a, where beams of light from a source fall upon two apertures and are combined in a telescope. The resulting image has a finite width and is shaped by effects including diffraction at the mirrors, and the bandwidth of the radiation. Maxima in the light intensity resulting from interference occur at angles θ for which the difference Δ in the path lengths from the source to the point at which the light waves are combined is an integral number of wavelengths at the effective center of the optical pass-band [1].

If the angular width of the source is small compared to the spacing in between adjacent maxima, the image of the source is occulted by alternate dark and light interference fringes and the source is said to be unresolved. If, however, the width of the source is comparable to the spacing between maxima, one can visualize the resulting image as being formed by the superposition of images from a series of points across the source. The maxima and minima of

the fringes from different points do not coincide, and the fringe amplitude will be attenuated (as shown by the dotted lines in the Fig. 2b) and the source is said to be partially resolved [1].

Michelson's visibility is defined as,

$$V_M = \frac{\text{intensity of maxima} - \text{intensity of minima}}{\text{intensity of maxima} + \text{intensity of minima}}$$

The fringe Visibility as described by Michelson is a completely real term, and a visibility value of 1, meant that the source of interest is completely unresolved as shown by the continuous lines in Fig. 2b and anything less than that would be partially resolved as shown by the dashed lines in Fig. 2b for visibility value of 0.5.

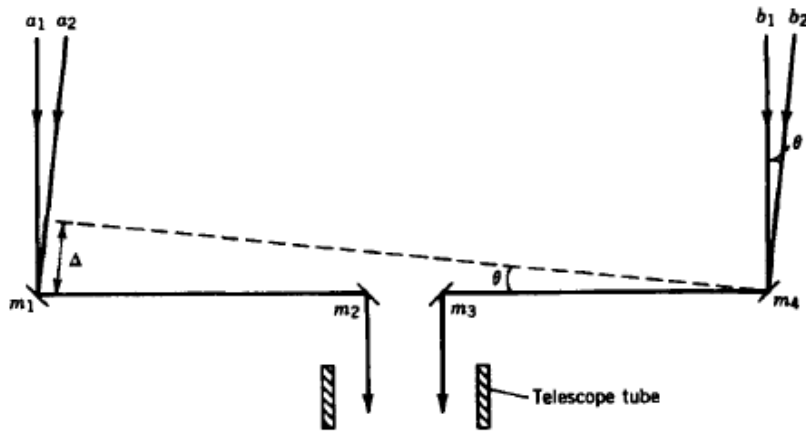


Fig.2a. Illustration of Michelson-Pease Stellar Interferometer, where, Light falls on the two extreme mirrors which are inclined parallel to their respective inner mirrors which guide the light onto the two slits, and a screen placed below the slits will have the interference pattern. [1]

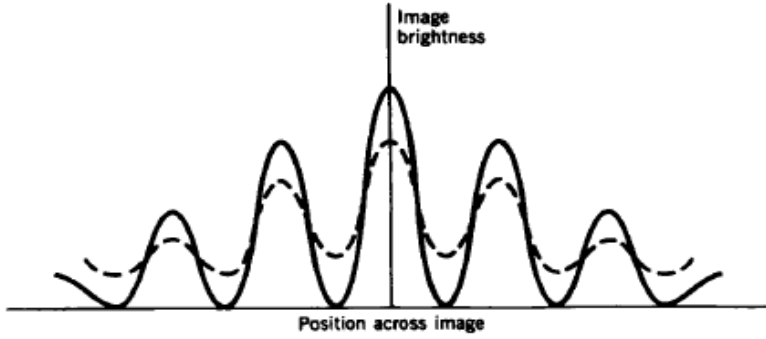


Fig.2b. Intensity of image as a function of position angle in a direction parallel to the spacing of the interferometer apertures. The solid line is the response of a source that is completely unresolved like a point source as per Michelson's Visibility equation and, $V_M = 1$. The dashed lines are the result of a comparable angular structure and in this case $V_M = 0.5$ and the source is partially resolved. [1]

By analogy to the double slit experiment, regions which would cause constructive and destructive interference, the response of an interferometer can be considered as “stripes” in the sky and the two slits are analogous to two antennas.

When two antennas are looking at a certain direction in the sky, we can assume the wave front to be parallel for sources at a large distance, and antennae will receive signals that are delayed (shifted in phase) as a function of the physical distance between them and the direction of the source with respect to the plane consisting of the antennas, at a particular observing wavelength (over the range of frequencies around the center frequency). Here the distance between the two antennas is termed as a Baseline, and our resolution equation can now be modified as, $R = \lambda/B$ where, B is the Baseline. A system with say 'n' antennae will have nC_2 different baselines associated to it.

2.2.3 A simple two element Antenna Interferometer

There are basically two types of interferometers, i.e. Adding type interferometer and Multiplying type interferometer.

In the Adding type, the two antenna outputs are added together and then squared. This results in the sum of squares along with the product term. The sum of squares can contain correlated noise terms from both the antennas. The Multiplying type only gives out the product term and hence is relatively noise free, and it is this type that we consider here.

Consider an antennae spacing in the east-west direction. The two antennas are separated by a distance D , the baseline, and observe the same source. The output of the two antennas are multiplied together to form the output of this interferometer. The source will be assumed to have infinitesimal angular dimensions and the receivers have narrow band pass filters.

The wave front from the source in direction θ reaches the right-hand antenna at a time,

$\tau_g = D/c \sin \theta$, before it reaches the left-hand one. τ_g is called the geometric delay and c is the velocity of light. Thus, in terms of the frequency ν , the output of the multiplier is proportional to

$$F = \sin(2\pi\nu t) \cdot \sin 2\pi\nu(t - \tau_g)$$

When the above output is passed through a Low Pass Filter or Integrator, then all the high frequency varying terms are filtered out and the output will yield the fringes

$$F = \cos(2\pi\nu\tau_g) = \cos\left(\frac{2\pi D l}{\lambda}\right)$$

Where, $l = \sin\theta$ is the direction cosine of the source's phase center with respect to the local E-W direction.

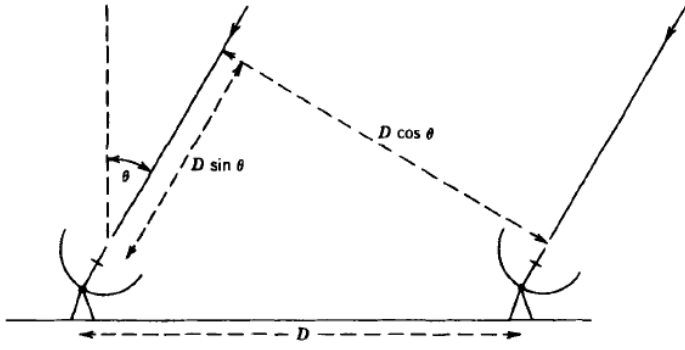


Fig.3. A simple two element interferometer [1]

2.3 RELATIONSHIP BETWEEN INTENSITY AND VISIBILITY

A commonly used (but not universal) co-ordinate system is one where the baseline vector is specified by (u, v, w) co-ordinates. Where w is chosen towards the phase tracking center which is the center of the source we wish to track, u is towards east and v is towards north and are measured in wavelengths. Positions in the sky are represented in (l, m) co-ordinates, which are the direction cosines measured with respect to the u and v axes.

The Michelson interferometer, seen earlier, measures the intensity only projected onto the l

direction, that is, the one-dimensional profile $I_1(l)$ given by

$$I_1(l) = \int I(l, m) dm$$

The phase of the fringe pattern, as well as the amplitude, varies with antenna spacing and must be measured to allow the intensity profiles to be recovered. To accommodate both fringe amplitude and phase, Visibility is expressed as a complex quantity. Since source brightness or Intensity is a real quantity, by Hermitian symmetry, the visibility amplitude will be even symmetric and visibility phase will be odd symmetric.

To recreate an image in 2-D we need to know how it varies in a 2-D plane, i.e. along both u and v axis. Consider a baseline mapping a source as shown in the Fig 4. The complex visibility function of the antenna can be written as

$$V(u, v) = |V| e^{j\phi_v} = \int_{4\pi} A_N(\sigma) I(\sigma) e^{-j2\pi D_\lambda \cdot \sigma} d\Omega$$

Where, $\sigma = s - s_0$, s is the source direction and s_0 is the chosen phase center,

$A_N(\sigma) I(\sigma)$ is the intensity of the source $I(\sigma)$ modified by the normalized antenna beam width, $A_N(\sigma)$ (which is the fourier transform of the Shape of the Antenna aperture, i.e a square tile will lead to a Sinc shaped beam. So long as we consider looking only at a narrow patch of the sky (a patch which is small enough to lie along a plane), we can safely assume the sky's spherical surface to be planar. Also the antenna gain can be assumed constant and taken out of the above integral).

The Visibility as seen here has a complex representation, with $e^{-j2\pi D_\lambda \cdot \sigma}$ representing the fringe term which brings both the real (cosine) and the imaginary (sine) components together.

The phase term, $2\pi D_\lambda \cdot \sigma$ gives the sinusoidal variation of fringe as a function of baseline

D_λ and source positions, $\sigma = s - s_0$.

The output of the interferometer at the phase center where we consider a hypothetical point source to be present is,

$$r(D_\lambda, s_0) = \Delta v \int_{4\pi} A(\sigma) I(\sigma) \cos[2\pi D_\lambda \cdot (s_0 + \sigma)] d\Omega$$

This can be written in terms of the visibility as follows,

$$r(D_\lambda, s_0) = A_0 \Delta v |V| \cos(2\pi D_\lambda \cdot s_0 - \phi_v)$$

The component of the baseline in the direction of the phase center is represented by the w term and hence,

$$D_{\lambda} \cdot s_0 = w$$

$$D_{\lambda} \cdot s = ul + vm + w \sqrt{1 - l^2 - m^2}$$

It can be shown that,

$$d\Omega = \frac{dl dm}{\sqrt{1 - l^2 - m^2}}$$

Where, $\sqrt{1 - l^2 - m^2} = n$, is the third direction cosine which is measured with respect to the w .

$$V(u, v) = \int_{-\infty}^{\infty} \int_{-\infty}^{\infty} A_N(l, m) I(l, m) e^{-j2\pi D_{\lambda} \cdot \sigma} d\Omega =$$

$$\int_{-\infty}^{\infty} \int_{-\infty}^{\infty} A_N(l, m) I(l, m) \exp\{-j2\pi [ul + vm + w(\sqrt{1 - l^2 - m^2} - 1)]\} \frac{dl dm}{\sqrt{1 - l^2 - m^2}}$$

2.3.1 Delay Tracking

To keep the relation between the intensity and the brightness to a simple 2-D Fourier transform, we need to try and eliminate the w component of the baseline as much as possible so that the baselines lie along a plane and this is known as fringe stopping. Fringe stopping requires an addition of a delay to be added in one of the antennas in every baseline pair which ensures that the source photons travel an equal amount of time to be processed by either antenna in the pair.

Since the projection of baseline along the direction of phase center is the w component, if the w component is compensated for, by applying appropriate delays, then we can retrieve the amplitude and phase of visibility for the phase center by correlating the two signals.

In general, the equation for visibility reduces to a Fourier transform relation shown below

$$V(u, v) = \iint A(l, m) I(l, m) e^{-j2\pi(ul+vm)} dl dm$$

This is consistent with the van Cittert-Zernike theorem by which, visibility is the Fourier transform of the sky brightness. If the measurement of the visibility function is confined to a plane (i.e. the w component is made zero by suitably adding delays), or only a small part of the sky is considered (i.e l and m are kept small enough that the term $\sqrt{1-l^2-m^2}$ goes to 1 and is no longer a function of l or m and hence can be taken as a constant term out of the integration thus reducing it to a simple double integration) , then, $V(u,v)$ and $I(l,m)$ reduce to Fourier transform pairs.

$$V(u, v) \xleftrightarrow{FT} I(l, m)$$

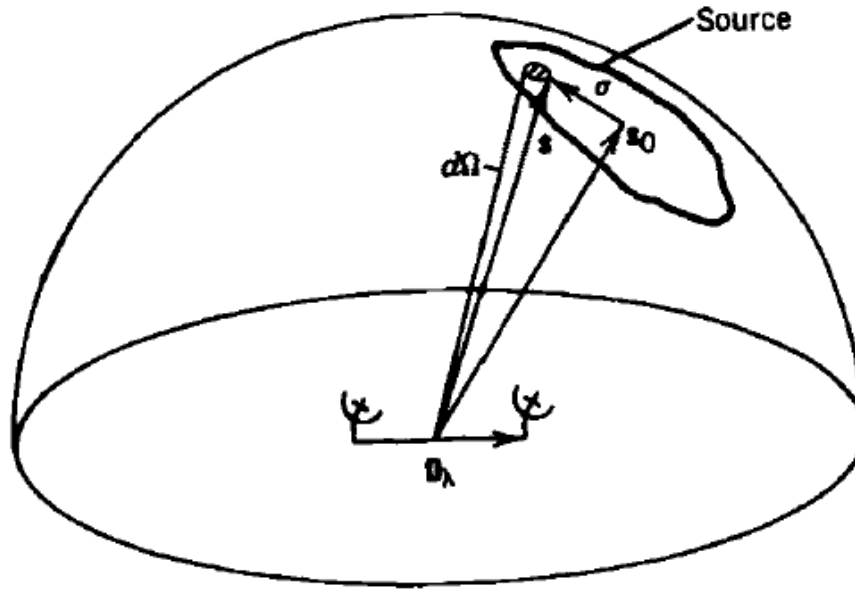


Fig.4. Baseline and source position vectors that specify the interferometer and source. The source is specified by the outline on the celestial sphere. [1]

2.4 ANTENNA ARRAY TELESCOPE

Earlier constructed Radio telescopes mostly used a single aperture Parabolic Dish Reflector, which is a relatively broad band antenna, and is mechanically steered to point to the source that was required to be observed. It has a feed at the point of focus if the dish at which all the waves underwent the same path length to constructively interfere. Although simple, it was required to have a very good robust design so that while steering, the dish should not collapse on the antenna mount due to its weight and the cost also was high owing to a lot of material to build the antenna.

There are two types of antenna arrays i.e. Phased Array and Correlator Array, with the difference being in the way they are interconnected as shown in Fig.5. The Phased Array power combines the outputs of the phase shifted antennas and then square law detects the combined signal such that their combined power is square of the sum of voltages out of the individual antennas, such that the output consists of both autocorrelation and cross-correlation terms. The power combiner is a matching network in which the output is

proportional to the sum of the radio-frequency input voltages. The Correlator Array on the other hand consists of multipliers that multiply all possible pairs of antenna outputs which give us only the cross-correlation terms.

Recently, the use of Array type telescopes have caught on, which are basically an array of cross dipole structures whose collective size should be the order of the size of a single aperture telescope that would have been employed for the same task, which reduces the cost of building the same. Also the beam of the antenna is electronically steerable by adding suitable delays to the dipole elements, so that it seems to be pointing in a certain direction in the sky (tracking the source). This eliminates the need for a mechanical mount, and the beam steering can be achieved much faster as compared to the parabolic dish type antenna.

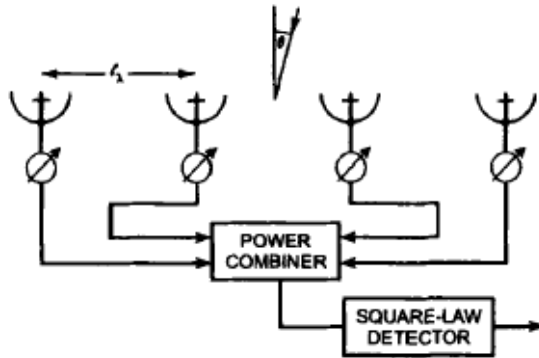


Fig.5a. Schematic of a Phased Array [1]

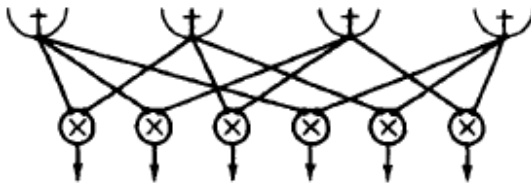


Fig.5b. Schematic of a Correlator Array [1]

2.5 EARTH ROTATION SYNTHESIS

The fact that the earth rotates around its own axis, gives us the ability to get different angles of source observation adding to the level of detail in imaging. The earth spins about its own axis at the rate of once every 23 hours 56 minutes 4 seconds, known as a Sidereal day, is shorter than the solar day by a degree and is the time over which the distant stars appear to appear at the same place locally with respect to the earth.

The Local Sidereal time is the time used to observe as well as timestamp all astronomical sources, which again is a function of the Longitude on earth. The Right Ascension and Declination of the sources are measured with respect to the point of crossing of the ecliptic plane (Plane containing earth's revolution around sun) and the equatorial plane (Plane perpendicular to the axis of rotation which passes through the poles) and where the Sun makes a relative transit from South to North with respect to the equatorial plane which is aligned at 23.5° to the ecliptic plane. This point is also known as vernal equinox or the first point of Aries. Hour Angle is a more useful measurement to determine current position of the source and is the difference of the Local Sidereal Time and the source Right Ascension. Given the Hour Angle and Declination of the source, the u,v,w can be found from the corresponding Cartesian coordinate measurement of the baselines.

We need to fix on an epoch or a time for our observations such that we timestamp our observations uniquely based on our location and for this we use Julian or Besselian epoch to express the current date as a single integer which gives the number of solar days from a remote period in history.

2.6 POLARIMETRY

Usually along with the Intensity information of a source, we are also interested in the polarization information. Polarization is synonymous to the polarization of the electric field

of the electro-magnetic wave. Two types of polarizations exist i.e. Circular and Linear or a combination of the two which manifests as Elliptical and everything else that does not belong to these categories is said to be randomly polarized. A source of interest sometimes consists of a combination of the above mentioned types which is measured in terms of a ‘degree’.

The measure of polarization that is almost universally used in astronomy is the set of four parameters introduced by Sir George Stokes in 1852. Within a single aperture antenna or a Phased array antenna, If the electric fields in the two orthogonal directions (for linearly polarized antennas) E_x and E_y are represented by $\mathcal{E}_x(t) \cos[2\pi vt + \delta_x(t)]$ and $\mathcal{E}_y(t) \cos[2\pi vt + \delta_y(t)]$, respectively, then the Stokes parameters are defined as follows:

$$I = \langle \mathcal{E}_x(t)^2 \rangle + \langle \mathcal{E}_y(t)^2 \rangle$$

$$Q = \langle \mathcal{E}_x(t)^2 \rangle - \langle \mathcal{E}_y(t)^2 \rangle$$

$$U = 2\langle \mathcal{E}_x(t)\mathcal{E}_y(t)\cos[\delta_x(t) - \delta_y(t)] \rangle$$

$$V = 2\langle \mathcal{E}_x(t)\mathcal{E}_y(t)\sin[\delta_x(t) - \delta_y(t)] \rangle$$

Where, the angular brackets denote the expectation or time average denoting an average over a time much longer than the coherence time $(\Delta\nu)^{-1}$, where $\Delta\nu$ is the bandwidth. This averaging is necessary because in radio astronomy we deal with fields that vary with time in a random manner, but have statistical properties of mean and variance which are deterministic.

Of the four parameters, I is a measure of the total intensity of the wave, Q and U represent the linearly polarized component, and V represents the circularly polarized component. If we measure the circular polarization of the E.M. waves, then V and Q give a measure of linear polarization whereas U gives a measure of circular polarization with sign, and I remains the same – as it is a measure of total polarization.

Stokes parameters I, Q, U, V measured using linearly polarized dipoles can be used to measure quantities such as:

$$m_l = \frac{\sqrt{Q^2 + U^2}}{I} \quad m_c = \frac{V}{I}$$

$$m_t = \frac{\sqrt{Q^2 + U^2 + V^2}}{I} \quad \theta = \frac{1}{2} \tan^{-1} \left(\frac{U}{Q} \right), 0 \leq \theta \leq \pi$$

Where, m_l , m_c , and m_t are the degrees of linear, circular, and total polarization, respectively, and θ is the position angle of the plane of linear polarization. For monochromatic signals $m_t = 1$ and the polarization can be fully specified by just three parameters. For random signals such as those of cosmic origin, $m_t \leq 1$ and all four parameters are required. When they are used to specify the total radiation from any point on a source, I, which gives a measure of the total intensity, is always positive, but Q, U, and V can take both positive and negative values depending on the position angle or sense of rotation of the polarization [4].

CHAPTER 3

RESEARCH METHODOLOGY AND EXPERIMENTAL SETUP

3.1 EXPERIMENTAL SETUP

The Setup for the system is defined in Fig. 6. and its various blocks and units are described below.

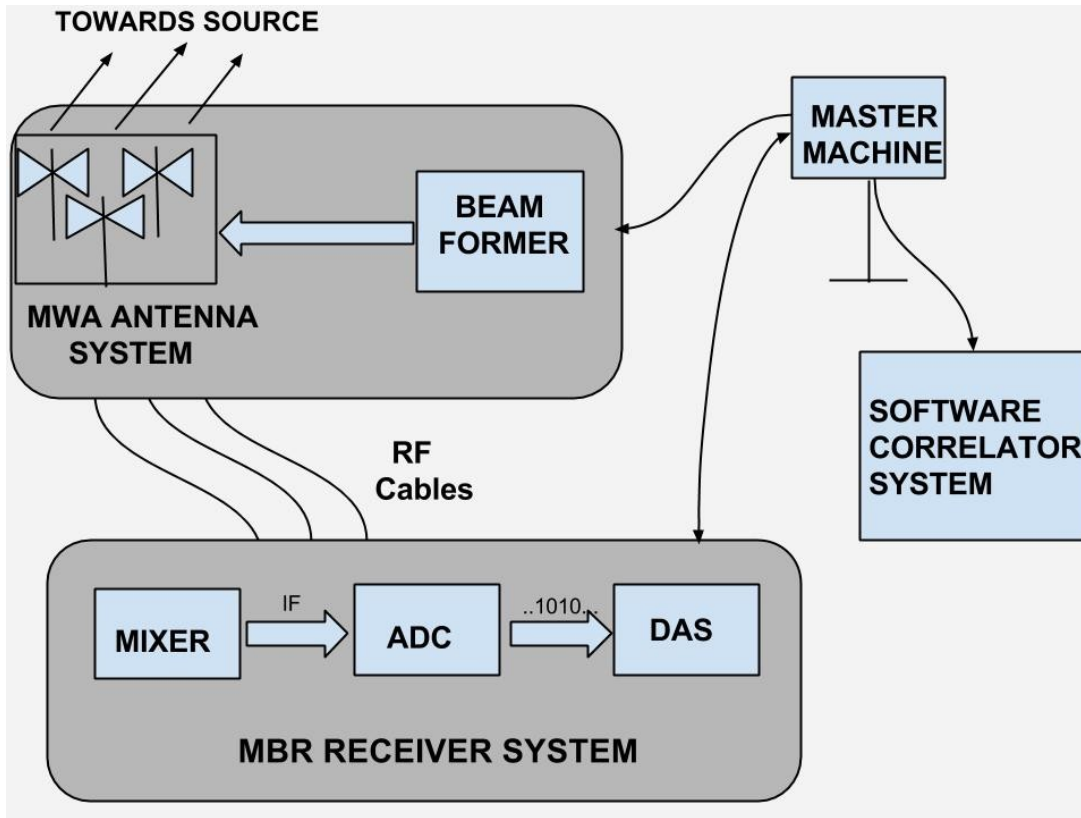


Fig. 6. Block diagram for the SWAN system

3.1.1 Murchison Wide-field Array Antennae (MWA)

The Antennae used in the experiment is borrowed from the Murchison Radio Observatory in Western Australia (Image 1), which consists of tiles of 4 X 4 Linear cross dipoles (i.e. a total of 16 cross dipoles), which have vertical bowtie elements that are symmetrical about the horizontal centerline, with an integrated LNA and Balun at the juncture between the two arms of the bowtie [2].

A Balun is a device which converts a balanced output of +V and -V volts to 0 and 2V volts. Field of view of a tile from the zenith is about 60°, and signals are combined in phase using a device called a Beamformer. The output of the cross dipoles are power combined into a single output per polarization which are then fed into a receiver after being appropriately mixed to the intermediate frequency of 140 MHz and down converted.

The tiles are placed on a 5m X 5m metallic ground plane which has structures smaller than the wavelengths of interest, and this acts as a reflector for these waves and at the feed we get a signal of stronger magnitude (i.e. Signal directly incident on the dipoles along with the signal reflected from the ground plane onto the dipoles). Each dipole consists of two Low Noise Amplifiers (LNAs) for each of the two polarizations, where the DC power for the LNA is carried by the Beamformer that is connected to the tiles. Each of these LNAs requires about 100mA of current and therefore across a single tile where we will have 32 dipoles – therefore 32 LNAs, we require about 3.2A of DC current. The MWA system has Minimal antenna gain at the horizon, to reduce terrestrial RFI that usually includes the FM and the TV bands [3].

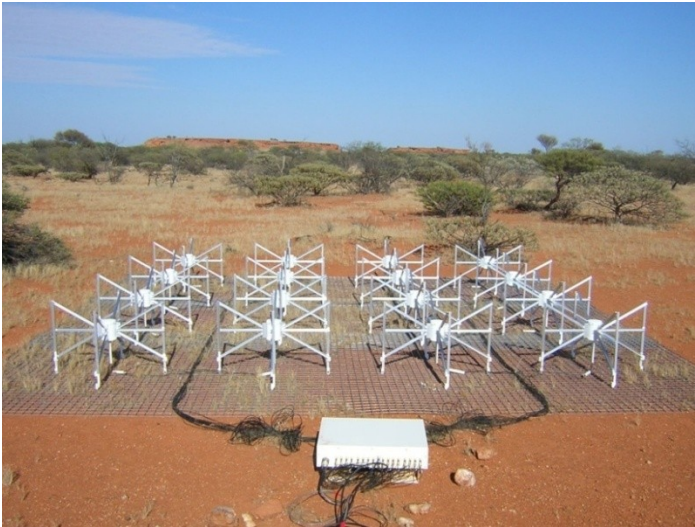


Fig.7. An MWA antenna tile image with a Beamformer

3.1.2 Beamformer

The beam-width is the area around the antenna where the signal can be received. The Beamformer is a device which is used for phasing or tilting electronically the antenna beam in a way that it appears to be looking at the source of interest directly.

Beam forming is done in order to get the best view of the source of interest in presence of background signal, and by having $N=16$ dipole elements, the signal to noise ratio of the tile

as an entity is improved by a factor of \sqrt{N} as the standard deviation of noise reduces by a factor of \sqrt{N} , which in this case leads to a factor of 4 improvement in the SNR.

The Beamformer box consists of 16 circuits to delay the RF signals emanating from each of the 16 cross dipoles (both polarizations delayed by the same amount) with a combination of 5 possible delay values in a binary fashion as shown below, which results in 32 distinct delay values.

If the 5 binary inputs are $I_4 I_3 I_2 I_1 I_0$ where I_4 is the most significant bit then,

$$\text{Delay at a cross-dipole} = I_4 * (16*D) + I_3 * (8*D) + I_2 * (4*D) + I_1 * (2*D) + I_0 * (D)$$

Where, D is the lowest value of delay that can be generated.

Each of the 16 cross dipoles are connected to a single beam former box which produces two RF outputs for the two polarizations, which are then fed to the receiver unit.

A program to control the beam formers exist where upon feeding the source Azimuth angle (subtended from the North direction) and Zenith angle (elevation angle subtended from the overhead direction), the delays are generated and fed to all the beam-formers which are interfaced via a beam-former interface box.

3.1.3 Multi-Band Receiver

The Multi-Band Receiver (MBR) has been borrowed from the Green Bank Telescope (GBT) at Green Bank in West Virginia, U.S.A. which is operated by the National Radio Astronomy Observatory (NRAO).

They consist of 10 dual receivers which have their independent Local Oscillators which are tuned at 10 relatively Radio Frequency Interference (RFI) free bands for the single dish at GBT, so that 10 bands between (100 MHz – 1500 MHz) can be observed simultaneously. But, in our system we require each of the receivers to be tuned at the same frequency as the aim of our system is to synthesize a large aperture from numerous uniform smaller apertures.

Each of the 10 receivers comes with a Local Oscillator (LO), an IF mixer module, a digital module which consists of two ADCs and a Data Acquisition System (DAS). The local oscillators work on the PLL principle and can be stepped in steps of 1 MHz, and based on the frequency value set via the master machine, the corresponding LO turns on. We split this LO frequency and feed it to all the receiver units. The IF mixer module translates the central frequency to 140 MHz based on the LO being generated. The reason 140 MHz is used is that the lower edge of the 16.5 MHz of the band coincides with the fourth harmonic of the sampling frequency 33 MHz, i.e. 132 MHz, and the technique used is called harmonic sampling.

This system also has RF and IF attenuation circuits for each of the polarizations that can be controlled from the master machine. The digital module houses the FPGA based 8-bit ADC circuit, which generates samples at the rate of 33 MHz per polarization and converts the data into the Ethernet packet standards adding 32 bytes of packet header to every 1024 bytes of dual polarized data packets. The synchronization and timing information of the system are taken care of by a GPS unit and a 10MHz reference clock signal. The GPS is used to discipline the 10MHz reference signal and also to maintain the network timing, so as to start the MBR recording on each of the DASes at the same instant of time. The Header byte of the packet contains a four byte packet sequence number field which is also very important for handling packet slips and maintain the timing correctly.

3.1.4 The MBR software system

The MBR system consists of the slave DAS systems controlled by a Master machine. There are commands to set various parameters like the Local Oscillator value in MHz, the name of the Source to be observed, Mode of observation, etc.

The individual terminal windows and the master terminal window can be brought up on the screen of the master upon start up of the master machine. Then we can set values that decide which of the DASes are going to be used, and which ones are going to be ignored. A command needs to be issued to set the attenuation levels at the RF output/IF input and at the IF output/ADC input, which is done so as to calibrate the gain levels across all the receivers. A command exists to program the FPGA unit inside the digital part of the receiver, which is responsible for the 8-bit dual channel Analog to Digital Conversion – which brings up an LED indicator against “TX” which indicates that the receiver is ready to record the data.

Once all the above boot up settings have been done, we can simply issue commands to start acquiring data on all the DASes, and we can provide the number of files to be recorded or the number of minutes for which data is to be captured as parameters where one minute is roughly equal to two MBR files of 2 GB each.

All of the DASes along with the master are connected via the switch, and it is through this that all the commands are issued. The data from the Digital module of each of the receivers are sent directly to the respective DASes via the other Ethernet port of the DASes. Once the files are simultaneously recorded from all the DASes, a bash script consisting of simple Linux commands can be run to transport the data from all the individual DASes into the master machine.

There is also a provision for running the acquisition in “sniff” mode, where 1 in every 1000 packets are sensed at the individual receivers are recorded on the master machine, and using a certain code, we can observe the data and check for any attenuation mismatches across the system.

3.2 SOFTWARE CORRELATOR SYSTEM BEING DEVELOPED

Cross correlation between two voltage sequences in time are related to the Cross spectra between them in frequency by a Fourier transform, for the response of the correlator in a radio interferometer, as shown below [1]

$$r(\tau) = \lim_{T \rightarrow \infty} \frac{1}{2T} \int_{-T}^T V_1(t) V_2^*(t-\tau) dt = V_1(t) \otimes V_2(t) \quad .$$

The above expression is the Time Cross Correlation which can be written in the form of convolution

$$V_1(t) \otimes V_2(t) = V_1(t) * V_2^*(-t)$$

Based on the Fourier relation for convolution, the above can be written as follows

$$V_1(t) \otimes V_2(t) \xrightarrow{FT} \tilde{V}_1(v) \cdot \tilde{V}_2^*(v).$$

As can be seen the Fourier transform of a convolution of two quantities is equal to the multiplication of the Fourier transform of the two quantities.

So we begin by calculating the cross spectrum of the signals which are the product combinations between the two polarizations of the two antennas in any baseline as follows

$$I_{xx} = V_{xi}(v) \cdot V_{xj}^*(v) \quad I_{yy} = V_{yi}(v) \cdot V_{yj}^*(v)$$

$$I_{xy} = V_{xi}(v) \cdot V_{yj}^*(v) \quad I_{yx} = V_{yi}(v) \cdot V_{xj}^*(v)$$

Where, V are the voltage values and the subscripts x and y denote the two states of polarizations and i and j denote the antenna numbers in the baseline. Note that these voltage values are all a function of frequency.

The Stokes Visibilities I, Q, U, V are related to the cross spectrum terms as follows

$$I = I_{xx} + I_{yy} \quad Q = I_{xx} - I_{yy}$$

$$U = \frac{1}{2}(I_{xy} + I_{yx}) \quad V = \frac{-j}{2}(I_{xy} - I_{yx})$$

Before going forward and plotting the obtained visibilities on the u-v plane, as a first exercise and a kind of sanity test, we wish to see the output Visibilities as a function of frequency which are changing every time block (which in this case is the integration time over which the samples are averaged). This has been shown in Image.2 below.

The filenames of the eight files, each belonging to a tile in the antenna system, are inputted through a text file, and point to a location on the internal or external disk where our data is present. Provision is made to check for and open the incremented sequences of these files if they exist.

FX style correlation is performed on the data in which the signal is first decomposed into its frequency components via a temporal Fourier transform. This results in a spectral channel consisting of the 16.5 MHz band with a bin size of about 60 KHz per bin in the case of 256 channels.

Product of the spectral channels of one antenna with the corresponding channel of the other antenna (cross correlations) and also with itself (auto correlation) are computed which give the cross spectra terms, and these are integrated (time averaged) over a certain number of samples as provided by the user, which removes noise and thus improves SNR.

A plotting routine that creates two kinds of plots is present for sanity checks,

1. Plot of averaged Amplitude vs. Frequency bin (lower triangle) and average Phase vs. Frequency bin (upper triangle) for every cross product in each of the baselines, except for autocorrelation which lies along the diagonal and consists of only the Amplitude plot (as the phase plot would yield zero and has no information).
2. Plot of amplitude averaged over a range of frequencies (specified by user) vs. time (lower triangle) and Phase averaged over a range of frequencies vs. time (upper triangle) for every cross product in each of the baseline, again with the exception of auto correlation whose amplitude plot is along the diagonal and has no phase plot.

The color coding of the cross spectra/stokes are given as below –

I_{xx}/I = Red

I_{yy}/Q =Blue

I_{xy}/U =Yellow

I_{yx}/V =Green

A baseline tracking routine exists, which calculates the source direction in terms of azimuth and elevation angles and which further calculates the direction cosines of l, m, n and further finds the dot product (projection) of these with the baseline components in u, v, w , which are expressed in units of wavelengths. This is the amount by which a delay needs to be added in a baseline pair so as to remove the w term, and ensure the signal is arriving at both the antennae at the same time (so to speak).

The FX correlator used for this purpose requires, the correction of the w term in two steps, i.e Coarse (Integral Delay Compensation) and Fine (Fractional Delay Compensation) correction [4]. As show in the diagram (Fig.8), the coarse delay is compensated for by delaying the time domain signals in steps of the sampling instant, this is achieved in program by simply wrapping around the samples that are delayed and then taking their Fourier transform after which the fractional delay is applied in the form of a phase gradient multiplied across all the frequency channels. Then each pair of these compensated output are complex multiplied and integrated over a suitable time which is at least a few times greater than the packet delay but less than the time over which the phase information is not lost much (when not tracking) and less than the time over which the baseline extent in the UV map has not changed from one point to the adjacent one.

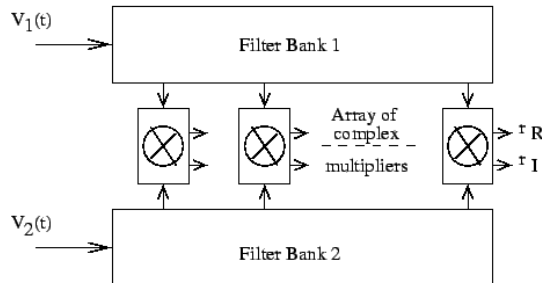


Fig.8a. Basic Block diagram of an FX type correlator as being used in the GMRT array [2]

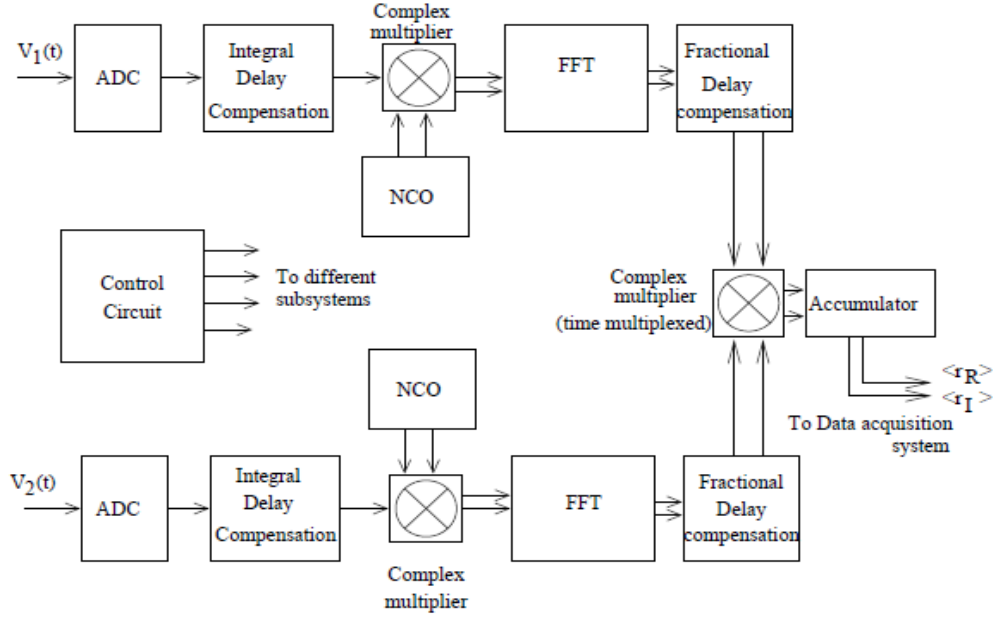


Fig.8b. Implementation of the FX style correlator as being used in the GMRT array [2]

3.2.1 Calibration technique for system and cable delays

A calibration table is created in order to account for the system delays and also the cable delays, which are connected between Antenna's and the observatory. Once the coarse delay correction is achieved, we are only left with a phase gradient that needs to be corrected. This can be achieved in the following way-

Once the cross terms are computed, they are Fourier transformed after zero padding (for oversampling) back into the time domain, where a Sinc shaped structure appears which has its peak shifted by an amount which represents the delay in the correlated pair. Since we are expecting the delays to exceed the length for which we take the Fourier transform, this method will work.

This is the delay present relative to the two systems. The Amplitude and Phase at the peak give the total power and the phase offset in the cross spectra respectively, which also needs to be corrected. Together these three values can be computed for the system in two scenarios,

1. Noise source input to estimate the system characteristics.
2. Point source (a real sky source) input to estimate the cable delays from antennas.

3.2.2 Local Sidereal Time

Once we know the Right Ascension and Declination of the source, we need to determine the local sidereal time which is location dependent, from which one can retrieve the Hour Angle of the source which changes as a function of time (Hour Angle = LST – Right Ascension). The Local Sidereal Time (LST) could be determined for our observation at the start of the correlation and can be tracked knowing the packet delays in seconds which can be converted to sidereal seconds.

Once we know this time we can calculate the path length that this direction makes with each of the antennae and hence the w term. This needs to be added appropriately to every pair in the nC_2 baselines to equalize the effective paths before correlating them.

When we are not tracking, i.e. only considering the central fringe, then the integration time must not exceed that time over which the w term changes more than a fraction of the wavelength at the center frequency being observed. If we are tracking the source then the integration time must not exceed the time after which any baseline moves from one point to a neighboring point in the UV map.

3.2.3 Coordinate systems

Knowing the source direction (phase reference), the l, m, n direction cosines can be determined. The u, v, w are the baseline vectors as seen by the source and this requires conversion of the local coordinates to the u, v, w values which is described below.

East North Up (ENU) to Earth Centered Earth Fixed (ECEF)

The antennae system is assumed to lie on a plane tangential to the surface of the earth. We need to fix a reference point on the plane which is the Array center. The distances to every antenna are measured along East North and Up topocentric coordinates with reference to the Array center. It is a convenient choice to assume one of the antennas as the Array center. We rotate this local coordinate system such that the Up axis is oriented parallel to the Earth's rotation axis (by rotating along the local east direction) and another rotation along the new Array Up axis by 90° such that the Array East now lies in the plane passing through the Local meridian reference. The resultant system is a kind of ECEF coordinate, except that Local East axis in the ECEF is pointing towards the Greenwich meridian rather than the local one.

If α is the latitude of the observer, then the required ECEF coordinates in wavelengths are,

$$\begin{bmatrix} X_\lambda \\ Y_\lambda \\ Z_\lambda \end{bmatrix} = \begin{bmatrix} 0 & \sin \alpha & -\cos \alpha \\ -1 & 0 & 0 \\ 0 & \cos \alpha & \sin \alpha \end{bmatrix} \begin{bmatrix} E \\ N \\ U \end{bmatrix}$$

ECEF to uvw system

The following equation is used for the conversion from ECEF to the uvw system,

$$\begin{bmatrix} u \\ v \\ w \end{bmatrix} = \begin{bmatrix} \sin H & \cos H & 0 \\ -\sin \delta \cos H & \sin \delta \sin H & \cos \delta \\ \cos \delta \cos H & -\cos \delta \sin H & \sin \delta \end{bmatrix} \begin{bmatrix} X_\lambda \\ Y_\lambda \\ Z_\lambda \end{bmatrix}$$

Where, H is the Hour angle of the source with respect to the plane passing through the observer

δ is the Declination of the source

$X_\lambda, Y_\lambda, Z_\lambda$ are the geocentric coordinates of the baselines expressed in units of wavelengths

and u, v, w are the source's projection on the baselines

3.2.4 The Dirty Map and Dirty Image

The u, v, w tags are the distances expressed in units of wavelengths and therefore vary across the bandwidth for a given baseline length and the phase reference position. The Visibilities measured are put on the Dirty map against the u, v values, and the scales on this map are made to half wavelength i.e. to add a suitable level of oversampling to satisfy the Nyquist criteria. Since every baseline can be associated in two ways where the counterpart visibility will have a complex conjugate value at the $-u, -v$. This inherently adds Hermitian symmetry to our uv plane, and by properties of Fourier transform, this gives us a purely real valued system in the transformed domain. A suitable coloring scale can be used to represent these real valued intensities of the Dirty Image.

3.2.5 Some challenges

Synchronization of data receivers

Every 15usecs a 1056 byte packet is generated in the Digital unit and is written into a binary file on the hard disk residing in the DAS. Sometimes these packets go unnoticed as the hard disk may fail to acknowledge them and they will not store the incoming packet, but thankfully the digital unit also puts a header of 32 bytes to all these packets that contains a 4 byte packet sequence number which can be thoroughly reliable. This means we cannot simply assume that the sequence of the data that gets recorded on the disk to be a continuous one and we must wait an integral number of packet time which is the difference between the received sequence and the expected sequence, whenever packets are missed.

There is also a possibility that GPS may not synchronize appropriately with all the digital receiver units and this may result in a misalignment of data within a packet, although the occurrence of this is rare, it is still found to have happened consistently in one of the receivers. As long as there is a consistency then we can account for these odd system behaviours.

Bandwidth effect

The signals that we observe are in a finite bandwidth of 16MHz of presumably constant amplitude and since a bandwidth consists of closely spaced fringe frequencies, the effect of that this has in the time domain are that these fringe cosines are shaped by a sinc function

which can be represented by the function $\frac{\sin(\pi \Delta \nu \tau)}{\pi \Delta \nu \tau}$, and this effect is especially more prominent at lower observing frequencies.

As a result of which, the maximum is obtained for $\tau = 0$, i.e. when the two time series, obtained from the same source with two antennas, are most coincident with each other at a given frequency. But if the geometric delay τ is a finite term then it will lead to a phase term introduced by the sinc nature of the envelope.

The Auto-correlation terms

Most existing array antennas only consider the nC_2 combinations of baselines which will all result in non-zero lengths in the $u-v$ plane, but there are also n autocorrelation terms which are present which are all located at the center of the visibility plane at all times. The problem with auto-correlating a signal which consists of various noise sources as a result of the sky background radiation, side lobes in antenna pattern, system noise, etc, is that the noise also gets correlated and hence at the end of each integration interval, the cross correlation would

be relatively more noise free as compared to the auto correlation terms. Yet we are interested in this parameter and we incorporate this in our visibility map to generate our image.

CHAPTER 4

RESULT ANALYSIS

A test white noise source is fed common to all the receiver systems, and in the spectral plots, as shown in Image 4a, a band in the region of frequencies (entered as input) will have a relatively flat response, its shape and the not so sharp cutoff are associated to non-idealities present in real system.

Ideally, the phase response as indicated by the upper triangle, should have been flat, but is not so due to different path lengths introduced by different cables connected to each of the receiver systems or even due to the system itself. This leads to a gradient (slope) in phases as, a shift in one domain leads to a phase gradient in the Fourier domain.

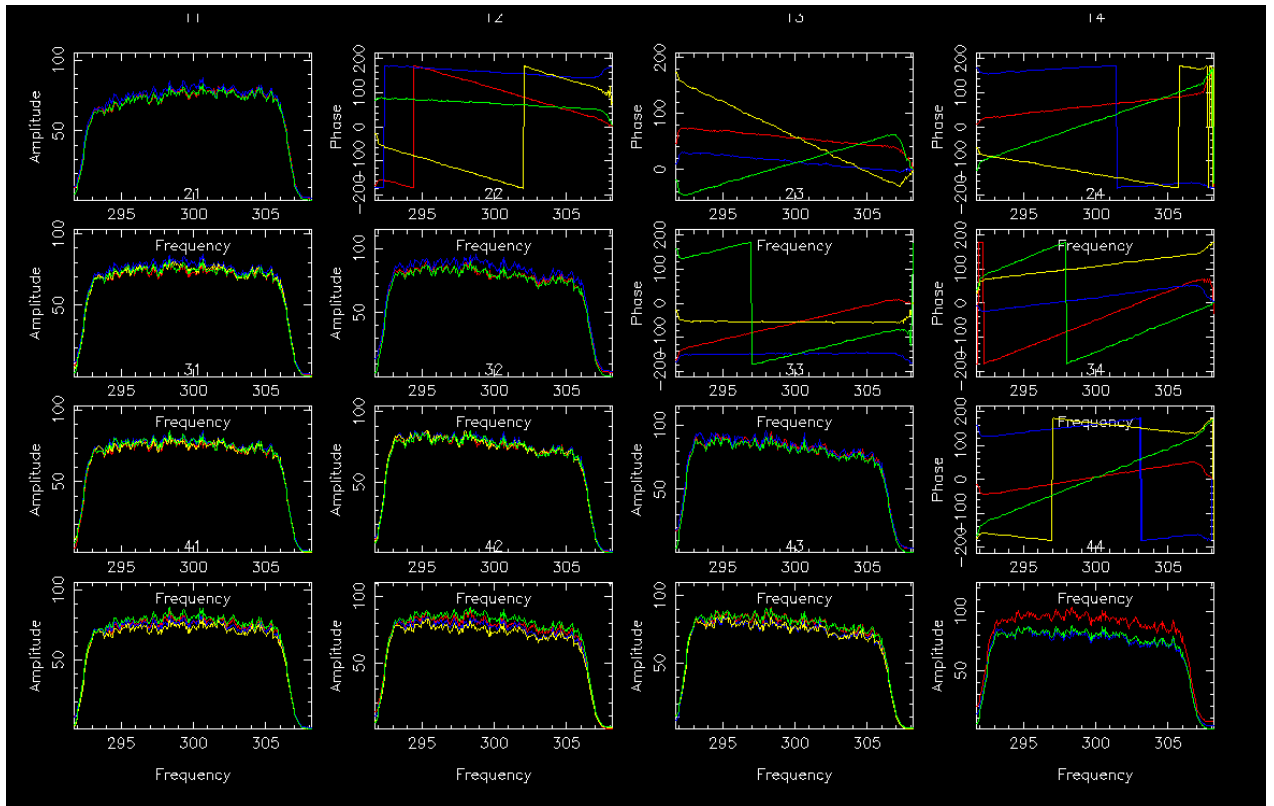


Fig.9a - A plot of the I_{xx} , I_{yy} , I_{xy} , I_{yx} cross products (lower triangle (cross correlations) and diagonal elements (autocorrelations)) and Phases (upper triangle) is plotted as a function of frequency (in MHz) for 4 antennae. Stokes products I , Q , U , V can also be plotted instead of the cross products.

A plot where the average of a band of frequencies over the averaging interval can also be a useful tool (Image 4b) to check if correlation level is maintained throughout our observation interval, and wherever the level is not maintained, that patch can be neglected for imaging. The X-axis gives the time elapsed in the data.

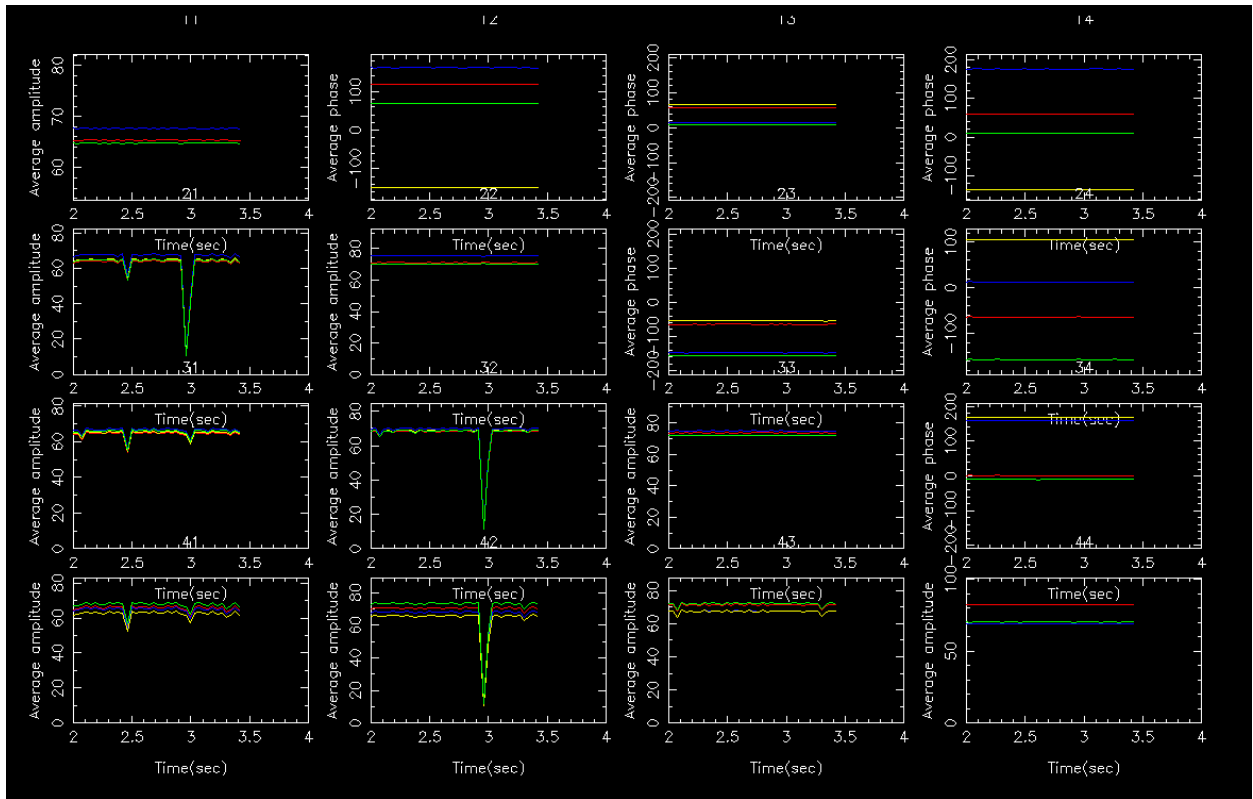


Fig.9b – The average power in a spectral band is plotted vs. time and for a point source. This can be used as a debugging tool.

The tool used to assess the system delays and compensate for them in a two step calibration process is as shown in Fig 10. This is obtained by taking the inverse Fourier transform of the cross products of the reference antenna with all the other antennae in the system (in this case antenna 1), and as a result of which we obtain the time cross correlation. The Fourier transform of a rectangular frequency band structure as expected will give us a Sinc in the time domain whose magnitude and phase have been plotted. The peak represents the maximum correlation between the 2 antennae and this gives us a measure of path difference introduced by the system.

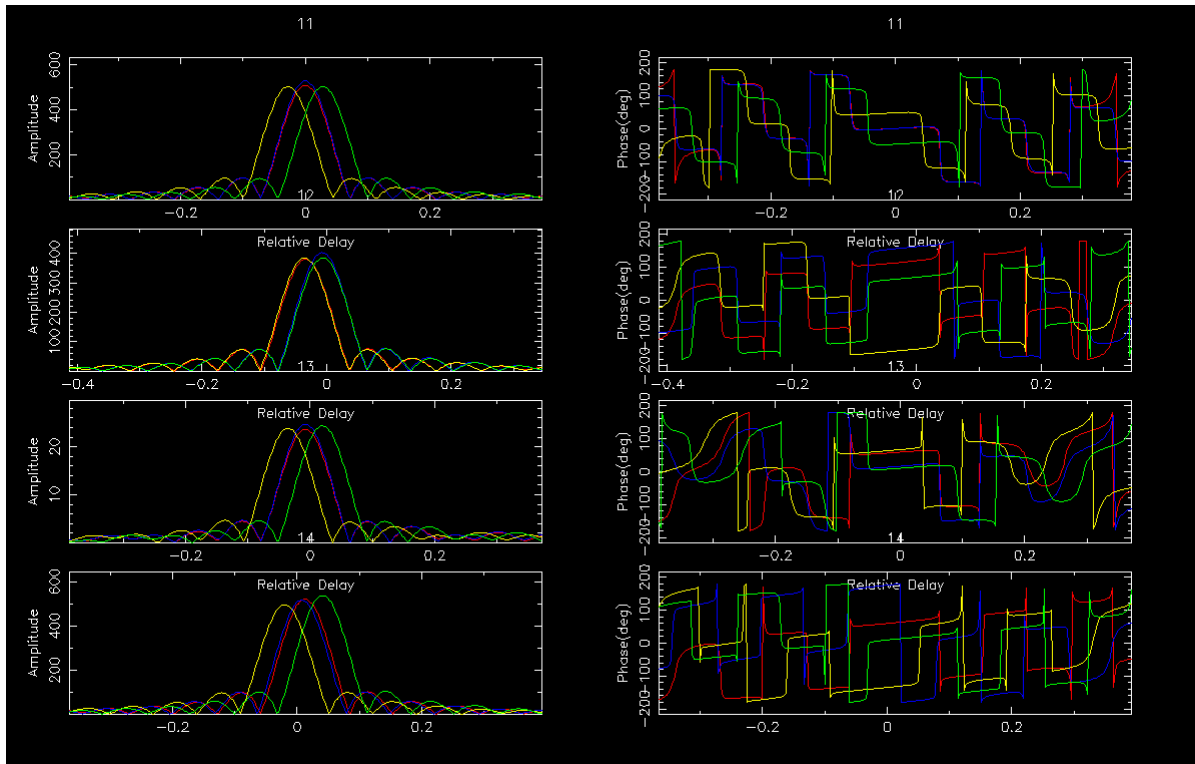


Fig10a. The left half of the plot gives the amplitude of the sinc function with respect to the relative delay (in microseconds). The right half gives the phase of the sinc (in degrees) with respect to the relative delay.

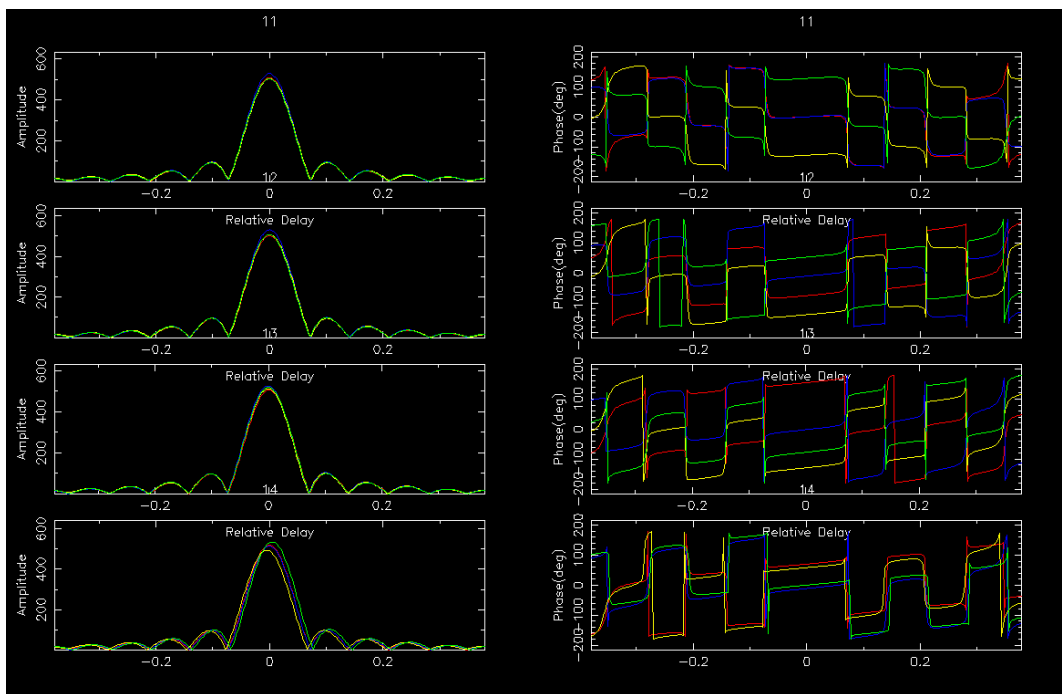


Fig10b. The relative delays (in microseconds) after compensation are reduced to zero and the phase offsets for Ixx and Iyy combination of cross products are also brought to zero.

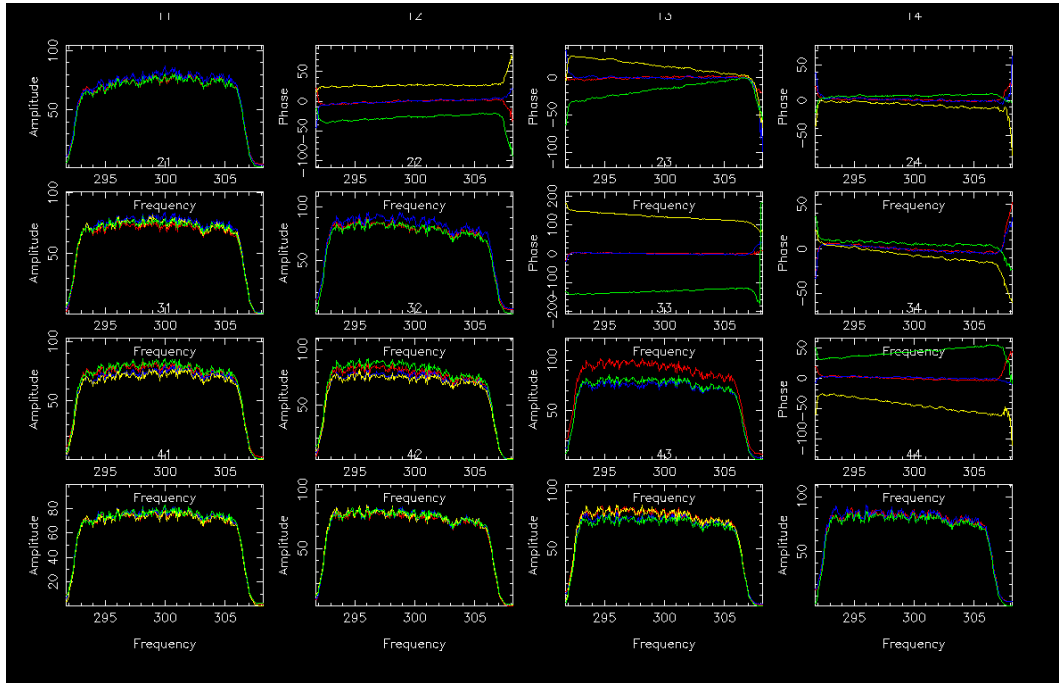


Fig.10c – After applying the delay calibration method, the phase gradients and offsets in Ixx and Iyy (Red and Blue) are removed completely, however possibly due to cross talk between the X and Y polarizations internally there still exists some gradient in Ixy and Iyx (yellow and green respectively).

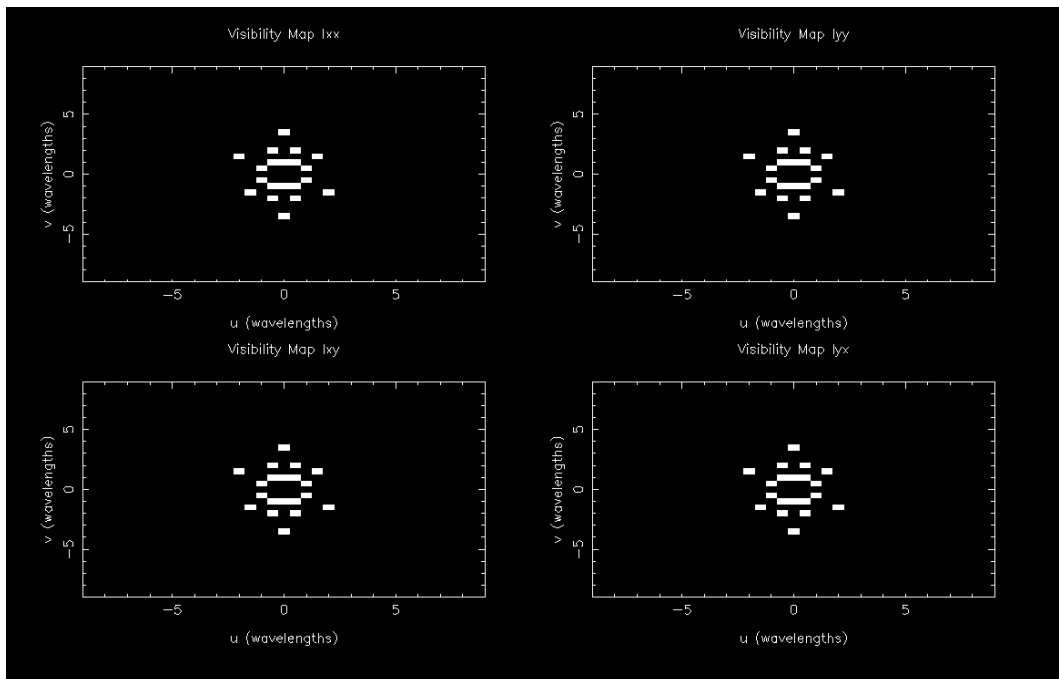


Fig11a. The dirty map represents the coverage of the baselines and this figure shows only a snapshot image. If we have a long observation of a few hours while the source is above the horizon then these points will form elliptical tracks.

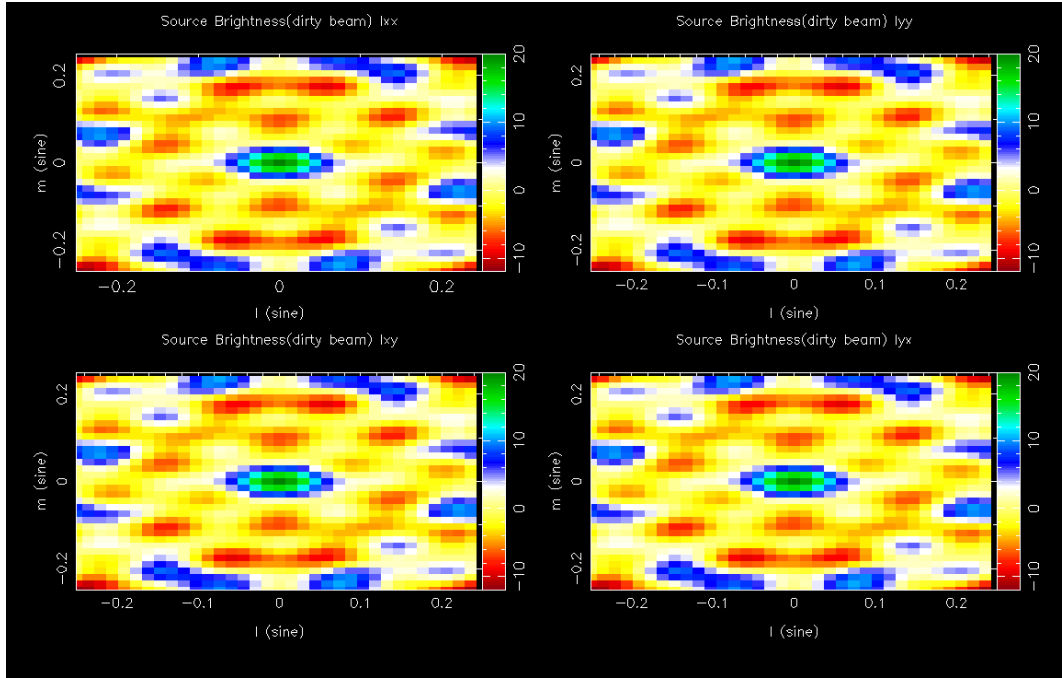


Fig11b. The dirty beam which gives the beam synthesized by the uv map, and is patchy due to incomplete uv coverage as seen in Fig. 11a.

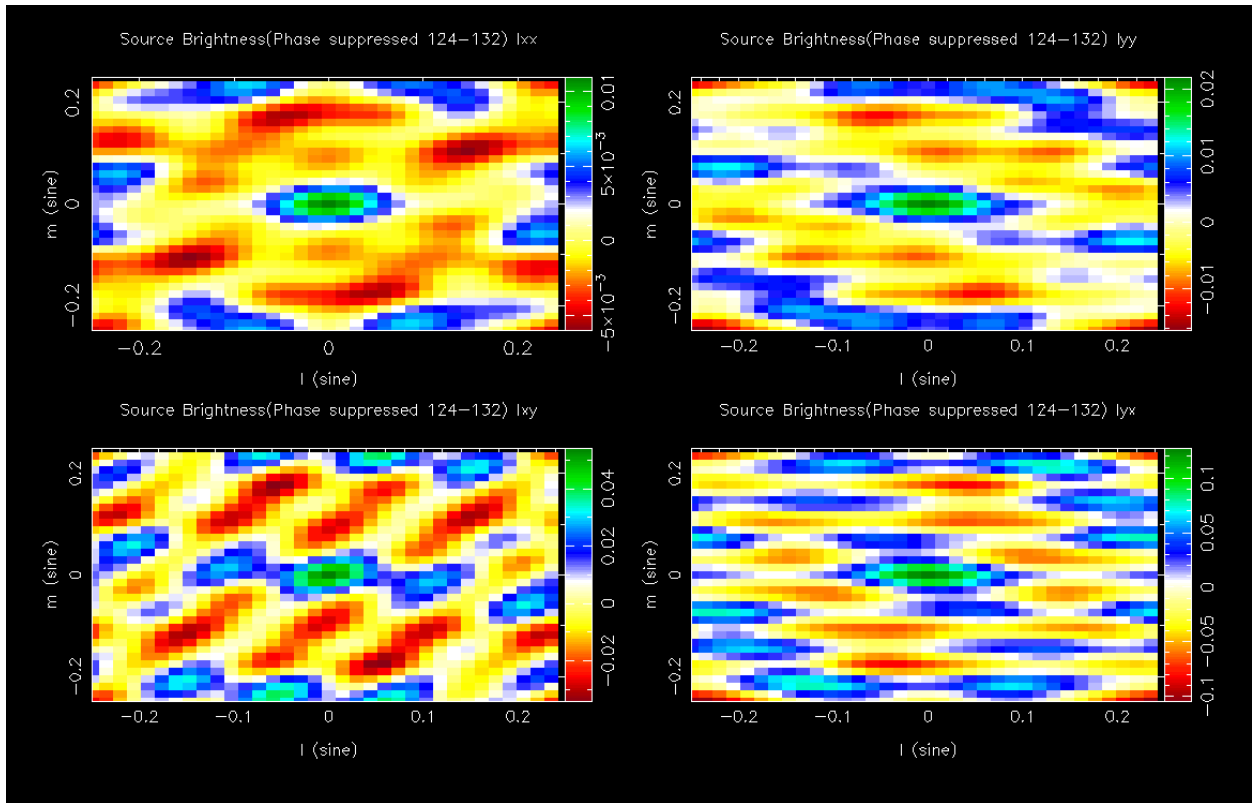


Fig12. A phase suppressed dirty image of the sun at mid band as observed with the system.

CHAPTER 5

CONCLUSION

This is a prototype system which is being developed in a small space initially to check feasibility. When elements from two different systems are combined together to create a new system then there is bound to be some mismatch, but an attempt has been made to address these difficulties.

A basic pipeline for Correlation and Synthesis imaging has been established, which can be used as a tool for debugging as has already been seen in the previous sections.

FUTURE SCOPE

The images obtained are shaped by effects due to lack of antenna coverage in the u - v domain, which acts like a multiplication of the true sky with a masking function given by the dirty map, and can also be thought of as a representation of the true sky convolved with the dirty beam. In order to remove this effect, certain deconvolution algorithms like CLEAN and Maximum Entropy Method (MEM) exist and will be invoked in future.

Although a basic function to output data into FITS (Flexible Image Transport System) format, for scientific imaging, has been created, a more advanced FITS routine will need to be written so that data can directly be used by astronomical tools such as AIPS, CASA, MIRIAD, etc.

A need for greater synchronization is required between the receivers and for this a common noise source power combined with the antenna signal will be fed to each of the receivers, such that at the start of any observation noise source may be switched ON and OFF for a small amount of time for calibration, since the noise source will be boosted in amplitude, it will overpower the astronomical signal during calibration data, and for the actual source observation, noise source will be switched off. This method will ensure the dynamically introduced delays in the system which are not due to cable delays may be mitigated.

REFERENCES

- [1] Thompson, A. R., Moran, J. M., & Swenson, G. W., Jr Interferometry and Synthesis in Radio Astronomy, J. Wiley, 1986.
- [2] http://gmrt.ncra.tifr.res.in/gmrt_hpage/Users/doc/WEBLF/LFRA/node3.html
- [3] Lonsdale, C.J. et al. "The Murchison Widefield Array: Design Overview." Proceedings of the IEEE 97.8 (2009): 1497-1506. © 2009 Institute of Electrical and Electronics Engineers
- [4] Maan, Y., et al. "RRI-GBT Multi-Band Receiver: Motivation, Design, and Development" 2013, ApJS, 204, 12
- [5] Kraus, J. D., Radio Astronomy (2nd edition), Cygnus-Quasar Books, 1986.
- [6] 'Young's double slit experiment' Illustration by Stannered ([File:Ebohr1.svg](#)) [CC BY-SA 3.0 (<http://creativecommons.org/licenses/by-sa/3.0>)], via Wikimedia Commons from Wikimedia Commons (file: http://commons.wikimedia.org/wiki/File%3AEbohr1_IP.svg)
- [7] 'Michelson Stellar Interferometer' Illustration by Alex-engraver (Own work) [Public domain], via Wikimedia Commons from Wikimedia Commons (file: http://commons.wikimedia.org/wiki/File%3AMichelson_stellar_interferometer.svg)
- [8] MWA tile image - <http://www.rigel.org.uk/blog/megan/images/dscn6314.jpg>

PROJECT DETAILS

<i>Student Details</i>			
Student Name:	RAHUL SURESH KINGER		
Register Number:	130915009	Section /Roll No:	DEAC
Email Address:	rahulkinger88@gmail.com	Phone No (M):	9964511776
<i>Project Details</i>			
Project Title:	DESIGN OF A CORRELATOR IN SOFTWARE, FOR SYNTHESIS IMAGING WITH A RADIO ASTRONOMY TELESCOPE ARRAY		
Project Duration:	12 MONTHS	Date of reporting:	7 th July, 2014
<i>Organization Details</i>			
External Guide:	Prof. Avinash Deshpande (email: desh@rri.res.in)		
Organization name with Full postal address and pin code:	Raman Research Institute CV Raman Avenue Sadashivanagar Bangalore - 560080, India		
Website address:	rri.res.in		
<i>Internal Guide Details</i>			
Faculty Name:	Dr. Mruthyunjaya HS		
Full contact address with pin code:	Professor, Department of Electronics and Communications, Manipal Institute of Technology, Manipal – 576104, Karnataka State, INDIA		
Email address:	mruthyu.hs@manipal.edu		